DOI: 10.1021/om100449t

ORGANOMETALLICS
Article

Structural Study of the Reaction of Methylzinc Amino Alcoholates with Oxygen

Nathan Hollingsworth,[†] Andrew L Johnson,[†] Andrew Kingsley,[‡] Gabriele Kociok-Köhn,[†] and Kieran C Molloy*,[†]

[†]*Department of Chemistry, University of Bath, Claverton Down, Bath, BA2 7AY, U.K. and* [‡]*SAFC Hitech, Power Road, Bromborough, Wirral CH62 3QF, U.K.*

Received May 10, 2010

Reaction of $ZnMe_2$ with 1,3-bis(dimethylamino)propan-2-ol (Hbdmap) in 2:1 ratio forms both [MeZn(bdmap)·$ZnMe_2$]$_2$ (**2**) and [MeZn(bdmap)]$_3$·$ZnMe_2$ (**3**) depending on the concentration of the reaction. In the former, $ZnMe_2$ is coordinated to a free N-donor of the bdmap ligand and rather more loosely to the oxygen of the alkoxide. In **3**, the $ZnMe_2$ is coordinated to two free N-donors of the bdmap ligand. **2** reacts with O_2 at low temperatures with controlled insertion into one of the Zn−C bonds of the coordinated $ZnMe_2$ group to form the peroxide [MeZn(bdmap)]$_2$MeZnOOMe (**4**). **4** decomposes slowly, and the hydroxide [MeZn(bdmap)]$_2$MeZnOH (**5**) was isolated; in addition to **5**, two other decomposition products have been unambiguously identified, namely, (MeZn)$_5$(bdmap)$_3$O (**6**) and (MeZn)$_4$(bdmap)$_4$ZnO (**7**). The formation of these species can be linked to reactions of the hydroxide (**5**), or its associated radical [MeZn(bdmap)]$_2$MeZn(O$^•$)], with species such as $ZnMe_2$ or MeZn(bdmap), present is solution as a result of operating Schlenk equilibria. The structure of [MeZn(bdmap)]$_4$ (**1**) is also reported.

Introduction

The reaction between ZnR_2 (R = Me, Et) and oxygen has a history dating back over 150 years since the early experiments of Frankland.[1] The products of this reaction have variously been suggested as the alkoxides RZn(OR) and Zn(OR)$_2$ or the peroxides RZn(OOR) and Zn(OOR)$_2$[2−6] with insertion of O_2 into either one or both Zn−C bonds; more recent reports have isolated cubanes [RZn(OR)]$_4$ and also bis-heterocubanes [(RZn)$_6$Zn(OR)$_8$] from these reactions, in which the presence or absence of water is influential of the outcome.[7] The reactions are generally uncontrollably fast, and the interception of intermediates along the reaction pathway has proved challenging. The widely held belief concerning the mechanism of this reaction is that it is radical in nature[8] on the basis of the early work of Davies, who demonstrated that the autoxidation of $ZnEt_2$ was inhibited by a radical scavenger (galvinoxyl), though not the first stage of the reaction.[6] Furthermore, there are numerous alkylzinc-mediated reactions involving ZnR_2/air that also clearly involve radicals,[9] e.g., epoxidation of enones[10] and Reformatsky-type reactions.[11] Indeed, many of these reactions require *in situ* formation of a zinc peroxide in the presence of an amino alcohol auxilary ligand,[12] a system typified by that which is the focus of this paper.

Alternative insights into mechanistic aspects of the ZnR_2/O_2 reaction have appeared over the last six years that have challenged the long-held assertion concerning a radical mechanism,[13,14] primarily through the work of Lewiński, who was first to structurally authenticate organozinc peroxides arising from O_2 insertion into a Zn−C bond. Thus, reaction of either EtZn(BDI) or EtZn(azol) with O_2 resulted in the isolation of the peroxides [(EtOO)Zn(BDI)]$_2$[15] and [(EtOO)Zn(azol)]$_2$[EtZn(azol)]$_2$,[16] respectively.

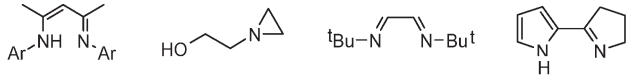

HBDI (Ar = 2,6-diisopropylphenyl) Hazol ^{t}BuDAB HPyr-pyr

Further work has demonstrated the importance of an equilibrium between four- and three-coordinate species i.e., $R_2Zn(L)_2 \rightleftharpoons R_2Zn(L) + L$ (L = N- or O-donor) in mitigating the rate of R−Zn/O_2 insertion. So, while $ZnBu^t_2$ reacts

*To whom correspondence should be addressed. E-mail: k.c.molloy@bath.ac.uk.

(1) Seyferth, D. *Organometallics* **2001**, *20*, 2940.
(2) Frankland, E. *J. Chem. Soc.* **1862**, *15*, 363.
(3) Lissenko, A. *Jahresber.−Inst. Hydrol., GSF-Forschungszent. Umwelt Gesund.* **1864**, 470.
(4) Demuth, R.; Meyer, V. *Ber. Bunsen-Ges. Phys. Chem.* **1890**, *23*, 394.
(5) Abraham, M. H. *J. Chem. Soc.* **1960**, 4130.
(6) Davies, A. G.; Roberts, B. P. *J. Chem. Soc. B* **1968**, 1074.
(7) Jana, S.; Berger, R. J. F.; Fröhlich, R.; Pape, T.; Mitzel, N. W. *Inorg. Chem.* **2007**, *46*, 4293.
(8) *Encyclopaedia of Inorganic Chemistry*; Grévy, J. M., Ed.; Wiley: Chichester, 2005.
(9) Akindele, T.; Yamada, K.-I.; Tomioka, K. *Acc. Chem. Res.* **2009**, *42*, 345.
(10) Porter, M. J.; Skidmore, J. *Chem. Commun.* **2000**, 1215.
(11) Mileo, E.; Benfatti, F.; Cozzi, P. G.; Lucarini, M. *Chem. Commun.* **2009**, 469.
(12) Enders, D.; Zhu, J. J.; Raabe, G. *Angew. Chem., Int. Ed. Engl.* **1996**, *35*, 1725.
(13) Lewiński, J.; Suwala, K.; Kubisiak, M.; Ochal, Z.; Justyniak, I.; Lipkowski, J. *Angew. Chem., Int. Ed.* **2008**, *47*, 7888.
(14) Lewiński, J.; Sliwinski, W.; Dranka, M.; Justyniak, I.; Lipkowski, J. *Angew. Chem., Int. Ed.* **2006**, *45*, 4826.
(15) Lewiński, J.; Ochal, Z.; Bojarski, E.; Tratkiewicz, E.; Justyniak, I.; Lipkowski, J. *Angew. Chem., Int. Ed.* **2003**, *42*, 4643.
(16) Lewiński, J.; Marciniak, W.; Lipkowski, J.; Justyniak, I. *J. Am. Chem. Soc.* **2003**, *125*, 12698.

 Published on Web 07/02/2010

rapidly with O_2 at −78 °C in THF to afford $[(THF)^tBuZn\text{-}OBu^t]_2$, the presence of methylpyridine (py-Me) requires reaction at −45 °C, and the peroxide $[(py\text{-}Me)^tBuZn(OO\text{-}Bu^t)]_2$ results.[14] The implications of this appear to be that the donor determines both the rate of formation of a three-coordinate intermediate by ligand dissociation (from a nominally four-coordinate precursor), and it is this coordinatively unsaturated center that is the reactive site; Zn−C bonds at a four-coordinate zinc are inactive to O_2 insertion. Presumably, the amino alcohol azole plays a similar role in the reaction of EtZn(azol) with O_2, which results in a product containing Zn−Et and ZnOOEt bonds in equal proportion.[16] These assertions have been supported in two further reports by Lewiński, in which N,N-chelating ligands (^{t}Bu-DAB, Pyr-pyr) have retarded the reaction of ZnR_2 with O_2 to afford examples of both tri- and tetrazinc clusters containing two ZnOOR functions.[13,17]

In this respect, the validity of interpreting the inhibition of the ZnR_2/O_2 reaction by radical scavengers as evidence for a radical mechanism has been questioned,[16] as these reagents could be influencing the course of the reaction by metal coordination, hence altering the coordination number.

Our own interest in the chemistry of zinc amino alcoholates has, serendipitously, given us an entry into this area of chemistry. We now wish to report a series of structural and NMR studies that relate to products from the reaction of $ZnMe_2$ with 1,3-bis(dimethylamino)propan-2-ol (Hbdmap) and that shed further light on the formation and evolution of organozinc peroxides.

Experimental Section

General Procedures. Elemental analyses were performed using an Exeter Analytical CE 440 analyzer. ^{1}H and ^{13}C NMR spectra were recorded on a Bruker Advance 500 MHz FT-NMR spectrometer as saturated solutions at room temperature, unless stated otherwise; chemical shifts are in ppm with respect to Me_4Si, and coupling constants are in hertz.

All reactions were carried out under an inert atmosphere using standard Schlenk techniques. Solvents were dried and degassed under an argon atmosphere over activated alumina columns using an Innovative Technology solvent purification system (SPS). Hbdmap[18] was prepared by literature methods.

Syntheses. Synthesis of $[MeZnbdmap.Me_2Zn]_2$ (2). Dimethylzinc (1 mL 2.0 M solution in hexane, 2.0 mmol) was added to Hbdmap (0.175 mL, 1.0 mmol) at room temperature, whereby an exothermic reaction took place and methane was evolved. On standing, colorless cube-like crystals appeared (1.09 g, 85%, mp 76 °C). Anal. Found (calc for $C_{20}H_{52}N_4O_2Zn_4$): C 37.7 (37.4), H 8.17 (8.16), N 8.58 (8.72). NMR (d_8 toluene 298 K), ^{1}H NMR: 3.72 (m, 2H, OCH), 2.07 (dd, 4H, J = 9.0, 12.9 Hz, CH_2N), 1.93 (s, 24H, CH_3N), 1.75 (dd, 4H, J = 2.3, 12.9 Hz, CH_2N), −0.82 (bs, 18H, CH_3Zn). ^{13}C NMR: 66.8 (CO), 65.0 (CH_2N), 45.3 (CH_3N), −12.2 (CH_3Zn).

Synthesis of $[MeZnbdmap]_2MeZnOOMe$ (4). Compound **2** (0.5 g, 0.78 mmol) was dissolved in hexane (1 mL) and stirred in an atmosphere of dry O_2 for 30 s, after which time the O_2 atmosphere was replaced with N_2. The solution was placed in a freezer overnight, whereby crystals of **4** formed (0.38 g, 84%, mp 101 °C). Anal. Found (calc for $C_{18}H_{46}N_4O_4Zn_3$): C 37.2 (37.4), H 7.84 (8.01), N 9.66 (9.68). ^{1}H NMR (d_8 toluene 298 K): 3.61 (m, 2H, OCH), 3.51 and 3.44 (2 singlets, 3H, OOMe), 2.06 (m, 4H, CH_2N), 1.89 (bs, 12H, CH_3N), 1.85 (bs, 12H, CH_3N), 1.63 (m, 4H, CH_2N), −0.74 (s, 3H, CH_3Zn), −0.78 (s, 3H, CH_3Zn), −0.82 (s, 3H, CH_3Zn). ^{13}C NMR: 66.4 (CO), 66.1 (CH_2N), 64.4 and 53.9 (OOCH3), 45.8 (CH_3N), −18.3 (CH_3Zn).

***In Situ* NMR Experiment.** Dimethylzinc (0.2 mL, 2 M solution in hexane, 0.4 mmol) was added to d_8-toluene (0.6 mL) in a Young's NMR tube. Hbdmap (0.035 mL, 0.2 mmol) was then added to this mixture in a nitrogen-filled glovebox. ^{1}H and ^{13}C NMR spectra obtained from this sample were identical to those of pure **2**. The headspace of the NMR tube was then filled with dry O_2 for 30 s, after which the O_2 was replaced with N_2. ^{1}H and ^{13}C NMR carried out on this sample were in agreement with that of **4** (albeit the MeZn region of the ^{1}H NMR spectrum was greater by 6H due to the unreacted Me_2Zn unit of **2**). The sample was then heated to 358 K over a 20 min period, kept at this temperature for 15 min, then cooled to 298 K, and the spectra were recorded down to 218 K to assess the decomposition of the peroxide (**4**).

Crystallography. Experimental details relating to the single-crystal X-ray crystallographic studies are summarized in Table 1. For all structures, data were collected on a Nonius Kappa CCD diffractometer at 150(2) K using Mo Kα radiation (λ = 0.71073 Å). Structure solution was followed by full-matrix least-squares refinement and was performed using the WinGX-1.70 suite of programs.[19] Corrections for absorption were made in all cases. Compound **1** crystallizes along with a molecule of hexane. For **3** there is half a molecule of toluene to every Zn complex, which was refined isotropically. Compound **5** crystallizes with half a molecule of toluene in the asymmetric unit, located about a center of inversion. In this structure, H(3), bonded to O(3), was located in the difference Fourier map and refined; however it was restrained to an ideal bond length. Furthermore, the ligand attached to both Zn(1) and Zn(3) in **5** was found to be disordered in the ratio 90:10; atoms with a lower occupation factor were refined isotropically. Compound **6** crystallizes with a molecule of toluene in its lattice and includes a disordered bdmap ligand, in which the CH_2 and NMe_2 carbons are split 70:30. For **7**, there is one molecule of toluene in the asymmetric unit. There is also disorder in the ratio 55:45 in one of the bdmap ligands; as a result, the bond length N(3)−C(13) was restrained.

Results and Discussion

We have previously reported on the reaction of ZnR_2 with the amino alcohols Hdmae, Hbdmap and Htdmap.[20]

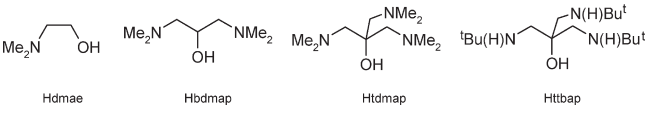

Reactions of both Hdmae and Htdmap proceed smoothly to give either tetrameric $[RZn(dmae)]_4$ or dimeric $[RZn(tdmap)]_2$ (R = Me, Et), respectively, as stable crystalline solids. In contrast, reactions with Hbdmap proved less straightforward.[20] A 1:1 reaction of $ZnMe_2$ with Hbdmap (4 mmol each reagent/total 20 mL toluene) resulted in only partial alkane elimination, unlike reactions with Hdmae or Htdmap, in which 1 equiv of CH_4 was liberated in both instances. When an excess of Hbdmap (2.2 equiv) was used, an oil analyzing as [MeZn(bdmap)] was finally isolated though NMR spectra did not allow any definitive structural information to be determined, while mass spectra indicated the presence of Zn_2−Zn_7 species present in the oil, on the basis of isotope distribution patterns. An aged sample of this oil has now yielded crystals of the

(17) Lewiński, J.; Suwala, K.; Kaczorowski, T.; Galezowski, M.; Gryko, D. T.; Justyniak, I.; Lipkowski, J. *Chem. Commun.* **2009**, 215.
(18) Campbell, K. N.; LaForge, R. A.; Campbell, B. K. *J. Org. Chem.* **1949**, *14*, 346.
(19) Farrugia, L. J. *J. Appl. Crystallogr.* **1999**, *32*, 837.
(20) Johnson, A. L.; Hollingsworth, N.; Molloy, K. C.; Kociok-Köhn, G. *Inorg. Chem.* **2008**, *47*, 12040.

Table 1. Crystal Data and Structure Refinement for 1−7

	1	2	3	4	5	6	7
formula	$C_{35}H_{87}N_8O_4Zn_4$	$C_{20}H_{52}N_4O_2Zn_4$	$C_{59}H_{140}N_{12}O_6Zn_8$	$C_{18}H_{46}N_4O_4Zn_3$	$C_{41}H_{93}N_8O_6Zn_6$	$C_{59}H_{140}N_{12}O_8Zn_{10}$	$C_{39}H_{88}N_8O_5Zn_5$
fw	945.61	642.14	1636.79	578.70	1186.45	1799.73	1076.02
cryst syst	monoclinic	triclinic	monoclinic	monoclinic	triclinic	monoclinic	orthorhombic
space group	$C2/c$	$P\bar{1}$	$P2_1/n$	$P2_1/c$	$P\bar{1}$	$P2_1/n$	$Pbn2_1$
a (Å)	18.0120(4)	8.0653(3)	21.5525(3)	8.2358(1)	9.0591(2)	17.9285(2)	9.8564(1)
b (Å)	15.0540(4)	9.5037(4)	8.3720(1)	20.3000(3)	13.1668(3)	9.4279(1)	20.8362(2)
c (Å)	36.528(1)	10.5151(5)	24.0648(4)	16.5998(3)	13.4498(3)	25.3635(3)	25.8918(3)
α (deg)		93.155(2)			73.491(1)		
β (deg)	97.679(1)	112.003(2)	102.068(1)	97.066(1)	72.678(1)	99.119(1)	
γ (deg)		100.315(2)			74.866(1)		
V (Å^3)	9815.8(4)	728.58(5)	4246.23(11)	2754.19(7)	1440.84(6)	4232.96(8)	5317.4(1)
Z	8	1	2	4	1	2	4
ρ_{calc} (mg/m^3)	1.280	1.464	1.280	1.396	1.367	1.412	1.344
μ(Mo Kα) (mm^{-1})	1.971	3.273	2.264	2.618	2.501	2.828	2.266
F(000)	4040	336	1732	1216	623	1884	2272
cryst size (mm)	0.30 × 0.20 × 0.03	0.40 × 0.25 × 0.08	0.20 × 0.20 × 0.20	0.30 × 0.15 × 0.10	0.20 × 0.20 × 0.10	0.25 × 0.15 × 0.15	0.23 × 0.20 × 0.20
θ range	2.93−27.49	3.24−27.53	3.75−27.46	3.08−27.49	3.21−27.51.	3.04−30.02	3.59−27.49
indep reflns [R(int)]	8171 [0.0810]	3338 [0.0705]	9621 [0.0836]	6294 [0.0997]	6582 [0.0532]	12 330 [0.0560]	11 000 [0.0717]
reflns obsd ($>2\sigma$)	4876	2672	6453	4411	5359	8659	8728
max., min. transmn	0.9432, 0.5893	0.7719, 0.3508	0.629, 0.629	0.7720, 0.5022	0.7880, 0.6346	0.6560, 0.5221	0.6600, 0.6238
goodness-of-fit	1.075	1.073	1.014	1.015	1.061	1.021	1.026
final R_1, wR_2 [$I > 2\sigma(I)$]	0.1064,0.2546	0.0424, 0.1014	0.0425, 0.0957	0.0423, 0.0949	0.0369, 0.0847	0.0393, 0.0721	0.0385, 0.0740
R_1, wR_2 (all data)	0.1739, 0.2878	0.0579, 0.1092	0.0797, 0.1093	0.0757, 0.1085	0.0515, 0.0922	0.0733, 0.0821	0.0615, 0.0815
largest diff peak, hole (e Å^3)	3.210, −0.749	0.792, −0.708	0.587, −0.777	1.523, −0.789	0.790, −0.686	0.500, −0.554	0.598, −0.351
Flack param							−0.003(10)

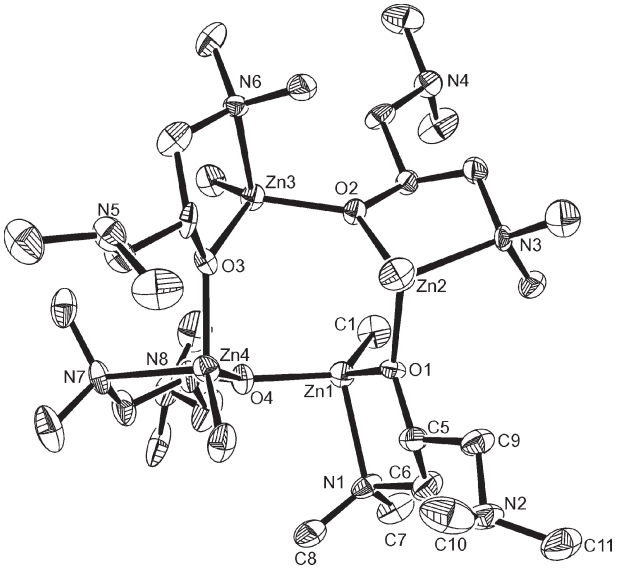

Figure 1. Asymmetric unit of **1** showing the labeling scheme used; thermal ellipsoids are at the 40% probability level. Selected metrical data (Å and deg): Zn(1)−C(1) 2.000(10), Zn(1)−O(1) 2.005(7), Zn(1)−O(4) 1.985(7), Zn(1)−N(1) 2.207(9); C(1)−Zn(1)−O(1) 124.7(5), C(1)−Zn(1)−O(4) 124.0(5), C(1)−Zn(1)−N(1) 112.5(5), O(1)−Zn(1)−O(4) 102.8(3), O(1)−Zn(1)−N(1) 84.5(3), O(4)−Zn(1)−N(1) 98.7(4) .

tetramer $[MeZn(bdmap)]_4$ (**1**) (Figure 1), which adopts essentially the same open cubane structure as $[MeZn(dmae)]_4$,[20] in which the additional coordination by the donor amine has weakened some of the intermolecular O:→Zn interactions.

While a 1:1 reaction of Hbdmap with $ZnEt_2$ does give [EtZn(bdmap)], this is also an oil consisting of species of undetermined nuclearity. Crystals of $[Zn(bdmap)_2\cdot Hbdmap]_2$ and $[EtZn_3(bdmap)_5]$ crystallize from these respective oils over a long period, suggesting Schlenk-type equilibria are operating:[20]

$$2RZn(bdmap) \rightleftharpoons ZnR_2 + Zn(bdmap)_2$$

For comparison, the corresponding cadmium species, RCd(bdmap), are trimeric solids.[21] Furthermore, when synthesizing a related cadmium compound with 1,3-bis(*tert*-butylamino)-2-(*tert*-butylaminomethyl)propan-2-ol (Httbap), [MeCd(ttbap)], a dimeric species with a molecule of $CdMe_2$ coordinated to the pendant N-donors, i.e., $[MeCd(ttbap)\cdot CdMe_2]_2$,[22] was isolated, which caused us to question why we had never seen analogous coordination chemistry among the organozinc amino alcoholates. As a consequence of these observations, we decided to look more closely at the $ZnMe_2$/Hbdmap reaction, initially with regard to its concentration dependence.

When $ZnMe_2$ and a sample of Hbdmap that had been handled in air were reacted in a 1:1 ratio but in a more concentrated manner (2 mmol each reagent/7 mL toluene) than in our previous work, the resulting solution yielded three distinct crystals, though resolution of the sample into analytically pure samples proved impossible. Crystallographic analysis of selected crystals showed that the reaction had resulted in a mixture comprising the adduct $[MeZn(bdmap)\cdot ZnMe_2]_2$ (**2**), the peroxide $[MeZn(bdmap)]_2MeZnOOMe$ (**4**), and a product likely to be a result of peroxide decomposition, $[(MeZn)_5(bdmap)_3O]$ (**6**); the formation of the peroxide most probably arises from the presence of oxygen in the Hbdmap sample used. In light of this serendipitous observation, we have looked more carefully at the course of this reaction.

First, using a degassed sample of Hbdmap and 2 equiv. of 2.0 M $ZnMe_2$ in hexane with no additional solvent added

(21) Johnson, A. L.; Hollingsworth, N.; Kociok-Köhn, G.; Molloy, K. C. *Inorg. Chem.* **2008**, *47*, 9706.
(22) Hollingsworth, N.; Molloy, K. C. Unpublished results.

Scheme 1

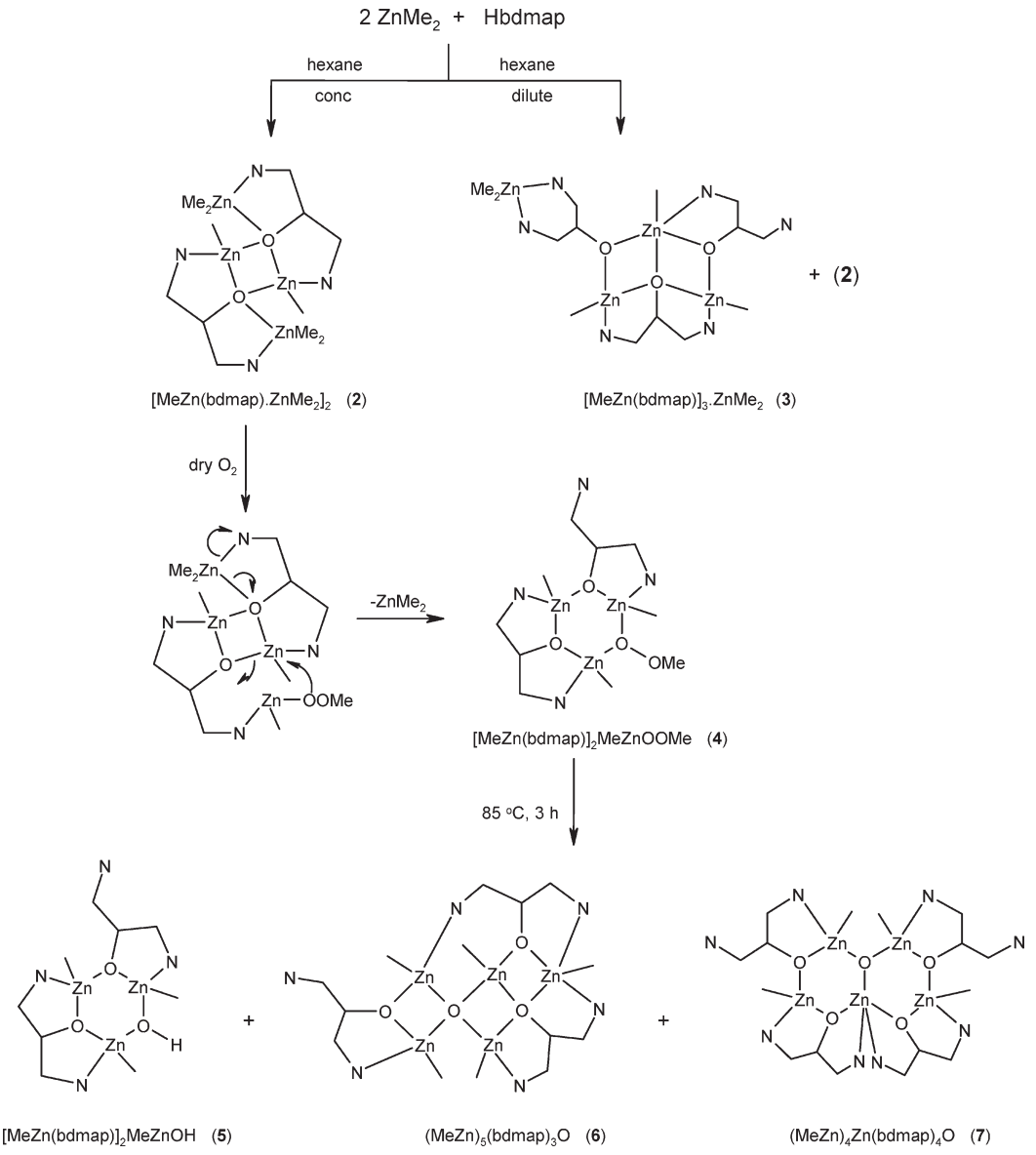

afforded the adduct $[MeZn(bdmap)\cdot ZnMe_2]_2$ (**2**) in 85% yield. When the reaction solution is diluted (2 mmol $ZnMe_2$ in 20 mL toluene) but retaining a 2:1 reaction stoichiometry ($ZnMe_2$:Hbdmap), the crystalline product again contains **2**, but a different adduct, $[MeZn(bdmap)]_3\cdot ZnMe_2$ (**3**), is also present. We have been unable to synthesize the latter adduct uniquely using a 4:3 reaction stoichiometry; if the solution is too concentrated, only **2** forms, while on significant dilution to avoid this problem, nothing crystallizes from solution (Scheme 1; N = NMe_2):

Compound **2** contains a dimeric $[MeZn(bdmap)]_2$ core (Figure 2) in which one arm of the amino alcohol acts as a κ^2-O,N bidentate donor to afford a four-membered Zn_2O_2 ring; each zinc has tetrahedral coordination similar to that seen in $[MeZn(tdmap)]_2$.[20] The free arm of the amino alcohol, along with oxygen of the Zn_2O_2 ring acts to coordinate a further equivalent of $ZnMe_2$ at each end of the dimer. The coordination sphere of the coordinated $ZnMe_2$ unit is a highly distorted tetrahedron, including relatively strong coordination to nitrogen [Zn(2)−N(2) 2.181(3) Å] along with a much longer interaction with the ring oxygen [Zn(2)−O(1) 2.773(2) Å]. The bond angles at Zn(2) are also very disparate, with the C(2)−Zn-(2)−C(3) [145.75(19)°] being particularly open. The structure of **2** is of the form described by Yamakawa and Noyori as the key intermediate in the addition of dialkylzinc to aldehydes, proposed on the basis of *ab initio* MO calculations.[23]

The ^{1}H NMR spectrum of **2** shows a single signal for the MeZn and Me_2Zn moieties, with a total integral of nine hydrogens (Figure 4a). At 238 K, this signal resolves itself so that both MeZn (3H) and Me_2Zn (6H) are discernible (Figure 4a, inset). The pattern of NMR coupling constants for the CH_2 protons of the bdmap ligand (two dd with J values rationalizable using the Karplus equation and the angles observed in the X-ray structure) is consistent with the ligand bridging between two metal centers, as we have previously seen with $[MeCd(bdmap)]_3$.[21]

The adduct $[MeZn(bdmap)]_3\cdot ZnMe_2$ (**3**), which forms along with **2** in more dilute solutions, incorporates a six-membered Zn_3O_3 ring but bonded across the ring [Zn(2)−O(3) 2.627(2) Å] to yield two fused four-membered Zn_2O_2 heterocycles

(23) Yamakawa, M.; Noyori, R. *J. Am. Chem. Soc.* **1995**, *117*, 6327.

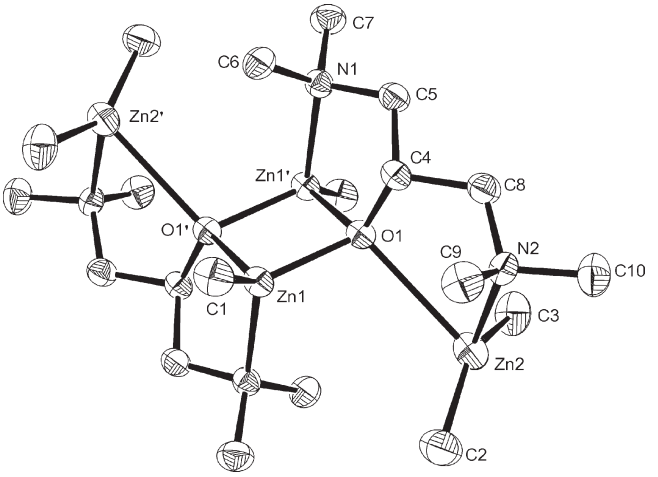

Figure 2. Asymmetric unit of **2** showing the labeling scheme used; thermal ellipsoids are at the 50% probability level. Selected geometric data (Å and deg): Zn(1)−O(1′) 2.102(2), Zn(2)−O(1) 2.773(2), Zn(1)−N(1′) 2.142(3), Zn(2)−N(2) 2.181(3); O(1)−Zn(1)−O(1′) 90.12(8), Zn(1)−O(1)−Zn(1′) 89.88(8), C(3)−Zn(2)−C(2) 145.75(19). Symmetry operation: $2-x$, $1-y$, $1-z$.

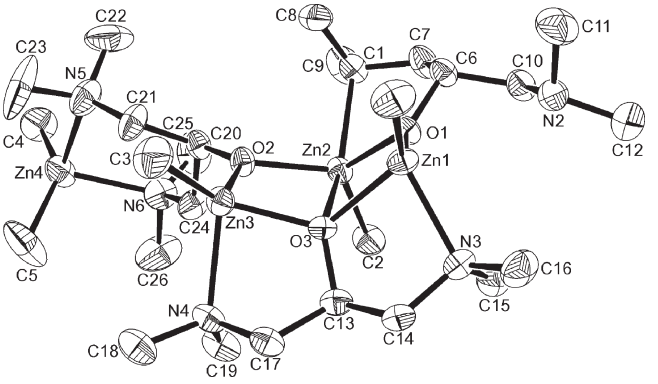

Figure 3. Asymmetric unit of **3** showing the labeling scheme used; thermal ellipsoids are at the 40% probability level. Selected geometric data (Å and deg): Zn(1)−O(1) 1.940(2), Zn(1)−O(3) 2.061(2), Zn(1)−N(3) 2.140(3), Zn(2)−O(1)1.989(2), Zn(2)−O(2) 2.008(2), Zn(2)−O(3) 2.627(2), Zn(2)−N(1) 2.296(3), Zn(3)−O(2) 1.987(2), Zn(3)−O(3) 1.990(2), Zn(3)−N(4) 2.232(3), Zn(4)−N(5) 2.230(4), Zn(4)−N(6) 2.233(3); O(1)−Zn(1)−O(3) 84.63(8), O(1)−Zn(2)−O(2) 116.39(9), O(2)−Zn(3)−O(3) 89.21(8), C(4)−Zn(4)−C(5) 139.37(19), Zn(1)−O(1)−Zn(2) 115.78(10), Zn(2)−O(2)−Zn(3) 109.35(9), Zn(1)−O(3)−Zn(3) 124.08(10).

(Figure 3). This structure is unusual, particularly in comparison with those of **4** and **5** (below), each of which have conventional Zn_3O_3 rings with *trans*-ring Zn−O interactions > 3.4 Å. Such open six-membered rings are known for organozinc alkoxides but are themselves relatively rare,[24] and the fused nature of **3** parallels that of the cadmium species $[MeCd(bdmap)]_3$, which we have reported recently.[21] Here, however, the preference of cadmium for coordination numbers greater than 4 makes the structure more expected. Both Zn(1) and Zn(3) in **3** are four-coordinated, with a $ZnCO_2N$ coordination sphere in which the Zn−O bonds are generally shorter [1.940(2)−2.061(2) Å] than in **2** [2.034(2), 2.102(2) Å], presumably due to steric congestion in the smaller ring. Conversely, the donor N:→Zn bonds in **3** tend to be weaker [2.140(3)−2.296 Å] than in **2** [2.142(3) Å].

(24) Hecht, E. *Z. Anorg. Allg. Chem.* **2000**, *626*, 2223.

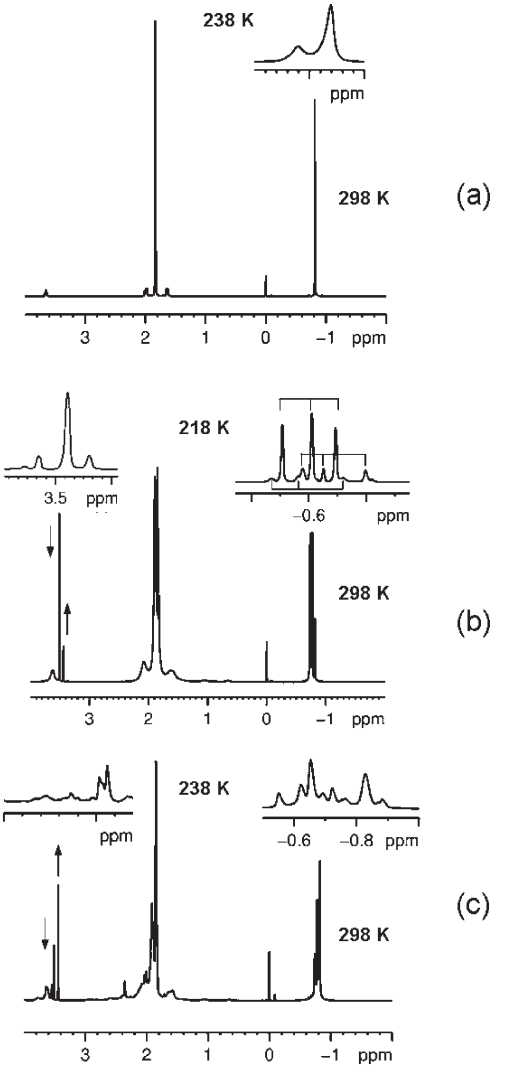

Figure 4. ^{1}H NMR spectra of (a) **2** at 298 K (inset at 238 K), (b) freshly dissolved **4** at 298 and (inset) 218 K, and (c) **4** after heating at 90 °C overnight, at 298 and (inset) 238 K.

Zn(2) on the other hand is five-coordinate ($ZnCO_3N$) as a result of the *trans*-ring Zn(2)−O(3) bond. There are three different bonding modes for the bdmap ligand. That based on O(3) is μ_3,κ^3-O,N,N, bridging Zn(1) and Zn(3) via oxygen supported by two additional N:→Zn bonds, along with a third, bridging Zn(2)−O(3) interaction. The ligand incorporating O(1) is μ_2,κ^2-O,N, with now only one N:→Zn supporting the Zn−O−Zn bridge. Finally, O(2) is simply μ_2 with respect to one of the four-membered Zn_2O_2 rings. This structural motif was one of our original suggestions for the structure of $[MeZn(bdmap)]_n$ based on NMR evidence, when the nuclearity of the oil was uncertain;[20] the isolation of tetrameric **1**, however, confirms that a complex mixture of oligomers is present in this oil.

In contrast to **2**, the $ZnMe_2$ adducted to the $[MeZn(bdmap)]_3$ trimer in **3** utilizes the two pendant nitrogen atoms of bdmap which is solely μ_2 with respect to the Zn−O rings [O(2)]. The coordination sphere of Zn(4) is more regular in terms of donor bonds [Zn−N: 2.230(4), 2.233(3) Å] than the $ZnMe_2$ adduct in **2**, though the C−Zn−C angle remains open [139.37(19)°]; clearly there are electronic rather than steric reasons for this behavior.

It is this coordination of $ZnMe_2$ to an oligomer $[MeZn(bdmap)]_n$, as evidenced in the structures of **2** and **3**, that we believe is the reason that 1:1 reactions of $ZnMe_2$ and

Hbdmap yielded only partial CH_4 elimination and required an excess of alcohol to form $[MeZn(bdmap)]_n$.[20]

When pure **2** is exposed to an atmosphere of dry O_2, an insertion reaction occurs to form the peroxide $[MeZn(bdmap)]_2$-MeZnOOMe (**4**) (Scheme 1). The IR spectra of both **4** and Hbdmap are rich in the region 800−900 cm^{-1} in which ν(O−O) might be expected, on the basis of published data for other zinc peroxides (813 w,[9] 854 m,[11] 868 m cm^{-1} [10]). Bands at 896 s and 811 w cm^{-1} , which do not coincide with bands in the spectrum of Hbdmap (876 m, 819 m cm^{-1} are the closest) are plausible candidates for this stretch. If, after exposure to the gas, the solution is kept at −20 °C to inhibit reaction, crystals of **4** can be isolated. The insertion of O_2 into one Zn−C bond can be seen quite clearly in the ^{1}H NMR spectra: addition of O_2 to a solution of **2** affords qualitatively the same ^{1}H NMR spectrum as that of a freshly prepared solution of pure **4** after isolation. The 298 K ^{1}H NMR spectrum of **4** (Figure 4b) shows three unequal MeZn singlets at −0.74, −0.77, and −0.82 ppm. In addition, a major singlet at 3.51 ppm, which we assign to the methylperoxo (MeOOZn) moiety, has appeared along with a weaker signal at 3.44 ppm, which we ascribe to the evolution of the peroxide into some other, so far unidentified, product(s), as it grows with time at the expense of methylperoxide signal. The total integral for the three MeZn signals and the two signals at *ca.* 3.5 ppm (MeOO + decomposition products) is 9:3, as expected for **4**.

The room-temperature ^{1}H NMR data for **4** become resolved and reveal a more complex picture at low temperature (218 K; Figure 4b, insets). The region associated with MeZn splits into what appears to be three 1:1:1 groups, the most intense of which (−0.51, −0.61, −0.69 ppm) must arise from **4**, as these are of an intensity that correlates them with the intense MeOO singlet at 3.48 ppm (shifted from 3.51 ppm at 298 K; integration, sum of signals at −0.51, −0.61, −0.69 to that at 3.48 ppm = 9:3); each of the singlets within this trio can be assigned to one of the three unique MeZn environments in **4**. Also, the growing singlet at 3.44 ppm, which we assign to either OMe or OOMe of a decomposition product(s) of **4**, resolves at 218 K into two singlets (3.53, 3.44 ppm) and a weaker, broader signal at 3.56 ppm. The latter integrates to 1H with respect to the weakest set of three singlets (−0.47, −0.56, −0.72 ppm), which have a relative intensity of 9H; that is, these signals are consistent with the hydroxide $[MeZn(bdmap)]_2MeZnOH$ (**5**), which we have isolated and confirmed crystallographically (see below). On the basis of integrals of the MeZn signals we estimate the ratio **4**:**5**: unidentified third (OMe) species to be ca. 70:10:20%.

Unfortunately, we have so far been unable to confirm the fate of the methoxy group, which we suggest must also arise from cleavage of the ZnO−OMe bond (see below), but a plausible suggestion is a methylzinc methoxide aggregate of some sort, such as $[MeZn(bdmap)]_2MeZnOMe$. However, the intermediate group of 1:1:1 signals (−0.58, −0.65, −0.80 ppm) have a total relative intensity of 9H with respect to the two signals at (3.53, 3.44 ppm), which each integrate to 1.5H, which therefore implies a structure in which two similar but nonequivalent methoxy groups are present, that is, more complex structurally than a simple Zn_3 species such as $[MeZn(bdmap)]_2MeZnOMe$.

Compound **4** is related to the trimeric $[MeZn(bdmap)]_3$ core of **3**, with one bdmap ligand replaced by the OOMe group (Figure 5). However, in this case (and **5**, below) the six-membered, non-planar Zn_3O_3 ring does not incorporate further *trans*-ring Zn−O bonds, and each metal center remains four-coordinate. Of the bdmap ligands that remain on going from **3** to **4**, one is μ_2,κ^3-O,N,N and the other μ_2,κ^2-O,N, as in **3**, while

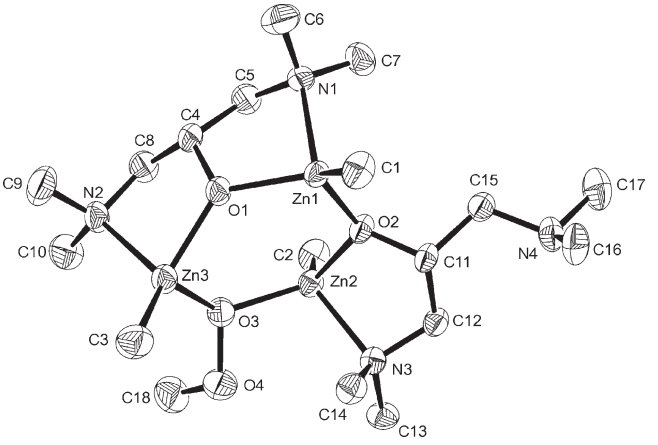

Figure 5. Asymmetric unit of **4** showing the labeling scheme used; thermal ellipsoids are at the 50% probability level. Selected geometric data (Å and deg): Zn(1)−O(1) 1.987(2), Zn(1)−O(2) 1.979(2), Zn(1)−N(1) 2.168(3), Zn(2)−O(2) 2.028(2), Zn(2)−O(3) 2.019(3), Zn(2)−N(3) 2.138(3), Zn(3)−O(1) 1.987(2), Zn(3)−O(3) 1.996(2), Zn(3)−N(2) 2.168(3), O(3)−O(4) 1.471(4), O(4)−C(18) 1.377(5); O(1)−Zn(1)−O(2) 98.85(10), O(2)−Zn(2)−O(3) 111.33(10), O(1)−Zn(3)−O(3) 92.10(10), Zn(1)−O(1)−Zn(3) 129.00(12), Zn(1)−O(2)−Zn(2) 123.46(12), Zn(3)−O(3)−Zn(2), 128.74(13), O(4)−O(3)−Zn(3) 115.8(2), O(4)−O(3)−Zn(2) 104.51(18).

the bond length data for Zn−O and Zn−N (Figure 4) are very close to those for **3**. The O−O separation in the peroxide [1.471(4) Å] is similar to data reported by others for zinc peroxides [e.g., 1.483(2),[16] 1.451(2) Å[15]].

The relationship between the dimeric precursor (**2**) and the trizinc final peroxide product (**4**) can be seen in the scheme for the reaction sequence (Scheme 1). In **2**, the weak bond between oxygen and one coordinated $ZnMe_2$ is easily broken, generating a reactive, three-coordinate zinc center. Oxygen, either as $MeOO^{\bullet}$ in a radical mechanism or O_2 in a concerted mechanism, is then able to react at this coordinatively unsaturated metal center. Coordination of the α-oxygen of the peroxide to a neighboring zinc of the strained Zn_2O_2 ring allows a ring opening to generate the six-membered Zn_3O_3 ring seen in **4**. Finally, it would seem reasonable that in the Zn_3O_3 ring in **4**, O, N chelation of $ZnMe_2$ is more crowded than in the Zn_2O_2 ring in **2**, and hence the second coordinated $ZnMe_2$ in **2** is released as the peroxide (**4**) is formed.

Allowing a solution of **2** exposed to dry O_2 to stand for several days at room temperature (rather than −20 °C) results in formation of **4** along with more extensive decomposition products, a process that can be replicated by heating a freshly prepared solution of **4** for 3 h at 85 °C (Scheme 1). This causes partial decomposition of the peroxide (diminution of the ^{1}H NMR signal at 3.55 ppm) while the signal at 3.44 ppm, arguably a methoxide decomposition product, grows. However, remarkably, at least some of the peroxide survives this treatment even after heating overnight (Figure 4c). The plethora of MeZn and MeO signals observable at low temperature (Figure 4c, inset) implies that the decomposition of the peroxide follows a number of routes; NMR signals due to $[MeZn(bdmap)]_2MeZnOH$ (**5**), $(MeZn)_5(bdmap)_3O$ (**6**), and $(MeZn)_4(bdmap)_4ZnO$ (**7**) (see below) are likely to be among them. While pure **4** seems more stable than previously reported organozinc peroxides, the presence of $ZnMe_2$ does seem to facilitate this decomposition. A solution containing $ZnMe_2$ and Hbdmap (2:1) (forming **2**), with O_2 added, which we have shown forms **4** *in situ* but with some

residual $ZnMe_2$ eliminated from the adduct, does, when heated overnight at 85 °C, afford complete decomposition of the peroxide, albeit accompanied by the formation of additional insoluble, and hence unidentified, by-products.

As discussed above, from a solution of **2** exposed to O_2 and heated at 85 °C for 3 h we have isolated three products in addition to the peroxide (**4**), though the reaction beyond the formation of **4** is not clean (Figure 4c) and none of the three species have been characterized other than crystallographically. Furthermore, no product contains an OMe (or new OOMe) function, which is implied by the change in the ^{1}H NMR spectrum of **4** around 3.5 ppm with time (Figure 4b,c).

We suggest compound **5**, $[MeZn(bdmap)]_2MeZnOH$, is formed from homolysis of the O−O bond in **4**. This decomposition route for main group metal peroxides has not been widely observed,[25,26] but is more common among transition metal analogues where oxidation of the metal can afford M=O species.[27] Recent work on organozinc peroxides has, however, argued convincingly for this mode of decomposition for zinc peroxides[17,28,29] and in one case the $MeO^{\bullet}$ radical generated by homoloysis of a ZnO−OMe bond trapped by judicious choice of co-ligand.[13] We assume that, in the absence of any other available radical, $[MeZn(bdmap)]_2MeZnO^{\bullet}$ scavenges $H^{\bullet}$ from the reaction solvent. It has recently been suggested that $RZnO^{\bullet}$ may abstract $H^{\bullet}$ from the departing $RO^{\bullet}$ followed by a 1,2-H shift in the resultant species,[29] though in our case we have no evidence for this through the formation of formaldehyde. Of course, in discussing the formation of **5** we cannot exclude the possibility that it is formed from hydrolysis involving adventitious moisture. However, the structural similarity of **4** and **5**, the retention of all the Me−Zn bonds during the course of the reaction (except where oxygenation has occurred), our isolation of zinc-oxo species **6** and **7** from these reactions, and the lack of any evidence for the formation of species of type $[MeZn(OR)]_4$ or $(MeZn)_6Zn(OR)_8$, which are commonly seen when $ZnMe_2$ reacts with O_2 in the presence of water,[7] are all consistent with the suggested O−O homolysis route.

The structure of **5** (Figure 6) is directly analogous to that of its precursor **4** in terms of ligation, with only minor changes in geometric data. Zn(1), not involved in bonding to either OOMe in **4** or OH in **5**, is essentially unchanged in the length of its Zn−O and Zn−N bonds. Both Zn(2) and Zn(3) are more weakly coordinated to their respective nitrogen donor atoms in **5**, due to replacement of OOMe with a less electronegative OH group, diminishing the Lewis acidity of the associated metal. In contrast, both Zn(2) and Zn(3) strengthen their bond to oxygen in **5** vs **4** [Zn(2)−O(3): 1.975(2) vs 2.019(3) Å; Zn(3)−O(3): 1.976(2) vs 1.996(2) Å], while the angle at O(3) is significantly narrower in the hydroxide [123.91(10)°] than the peroxide [128.74(13)°].

The second product associated with decomposition of the peroxide is the Zn_5 aggregate $(MeZn)_5(bdmap)_3O$ (**6**), a solid that melts at room temperature. Despite the structural relationship between **6** and its precursor **5**, there is a significant difference. The six-membered Zn_3O_3 rings present in

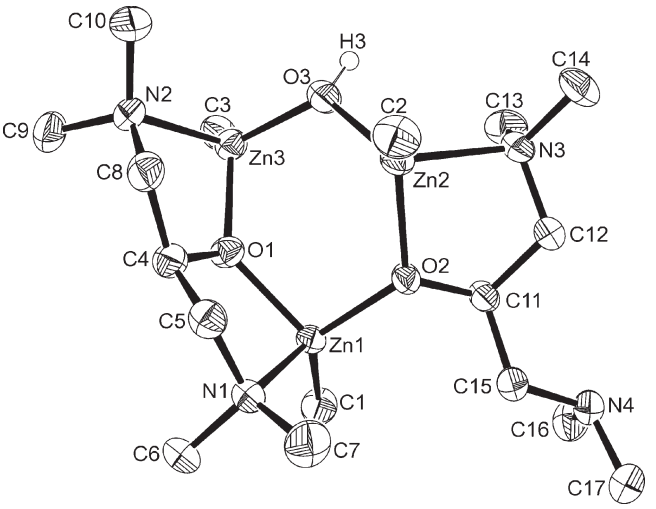

Figure 6. Asymmetric unit of **5** showing the labeling scheme used; thermal ellipsoids are at the 50% probability level. Selected geometric data (Å and deg): Zn(1)−O(1) 1.9862(18), Zn(1)−O(2) 1.9822(17), Zn(1)−N(1) 2.173(2), Zn(2)−O(2) 2.0232(17), Zn(2)−O(3) 1.975(2), Zn(2)−N(3) 2.175(2), Zn(3)−O(1) 1.9877(19), Zn(3)−O(3) 1.976(2), Zn(3)−N(2) 2.192(2) Å; O(1)−Zn(1)−O(2) 96.77(8), O(2)−Zn(2)−O(3) 108.53(8), O(1)−Zn(3)−O(3) 96.98(8), Zn(1)−O(1)−Zn(3) 126.27(9), Zn(1)−O(2)−Zn(2) 123.48(9), Zn(3)−O(3)−Zn(2) 123.91(10), H(3)−O(3)−Zn(3) 115(3), H(3)−O(3)−Zn(2) 113(3).

both **4** and **5** distort to form two fused four-membered rings in **6** (Figure 7), as also seen in **3**. This is done by forming a bond between Zn(2) and O(1) [2.0899(19) Å], which in **4** and **5** is a long, non-bonding separation [**4**: 3.138; **5**: 3.346 Å]; the two fused Zn_2O_2 rings in **6** have a structural parallel in the cadmium trimer $[MeCd(bdmap)]_3$.[21] The bdmap ligand based on O(1) remains μ_2,κ^3-O,N,N bridging Zn(1) and Zn(3), as it does in **4** and **5**, but the bdmap based on O(2) uses the free N-donor present in the two precursors to coordinate Zn(5) of the additional Zn_2 fragment of **6**, becoming μ_2,κ^3-O,N,N in the process. The final bdmap, which is part of the $(MeZn)_2(bdmap)$ fragment that has been incorporated into **6**, adopts a μ_2,κ^2-O,N coordination, leaving one Me_2N donor [N(6)] uncomplexed. The two halves of the molecule are centered on O(3), originating from the peroxide in **4** or hydroxide in **5**, which has tetrahedral μ_4-coordination. The Zn_4O motif is found in basic zinc salts such as $Zn_4(O)(O_2CMe)_6$[30] and has featured in the decomposition products of other organozinc peroxides.[17,28] All the zinc atoms in **6** are four-coordinated (as in **4** and **5**), except Zn(1), which expands its coordination number to five by interactions with two donor nitrogen atoms [N(1), N(3)].

Related to **6** is a second decomposition product, $(MeZn)_4Zn(bdmap)_4O$ (**7**) (Figure 8). This differs from **6** in having one zinc that is devoid of methyl groups and is a fusion of two six-membered Zn_3O_3 rings along a common edge. Each methylzinc is tetrahedral at the metal with $ZnCO_2N$, while the more Lewis acidic Zn(5) is five-coordinated (ZnO_3N_2 coordination). The Zn_3O_3 ring involving Zn(1), Zn(2), and Zn(5) is structurally analogous to that in the peroxide (**4**) or hydroxide (**5**), so that O(5) can be equated with the α-oxygen of the peroxide. The geometry about O(5) is trigonal planar and is a rare example of a planar μ_3-OZn_3 unit, others being {[pyr-2,5-Ph_2]Zn$(THF)_2$

(25) Kumar, S. S.; Singh, S.; Roesky, H. W. *Inorg. Chem.* **2005**, *44*, 1199.
(26) Li, H.; Song, H. B.; Duan, L.; Cui, C.-P.; Roesky, H. W. *Inorg. Chem.* **2006**, *45*, 1912.
(27) DiPasquale, A. G.; Kaminsky, W.; Mayer, J. M. *J. Am. Chem. Soc.* **2002**, *124*, 14534.
(28) Lewiński, J.; Bury, W.; Dutkiewicz; Maurin, M.; Justyniak, I.; Lipkowski, J. *Angew. Chem., Int. Ed.* **2008**, *47*, 573.
(29) Lewiński, J.; Kościelski, M.; Suwala, K.; Justyniak, I. *Angew. Chem., Int. Ed.* **2009**, *48*, 7017.
(30) Hiltunen, L.; Leskela, M.; Makela, M.; Ninisto, L. *Acta Chem. Scand. A* **1987**, *41*, 548.

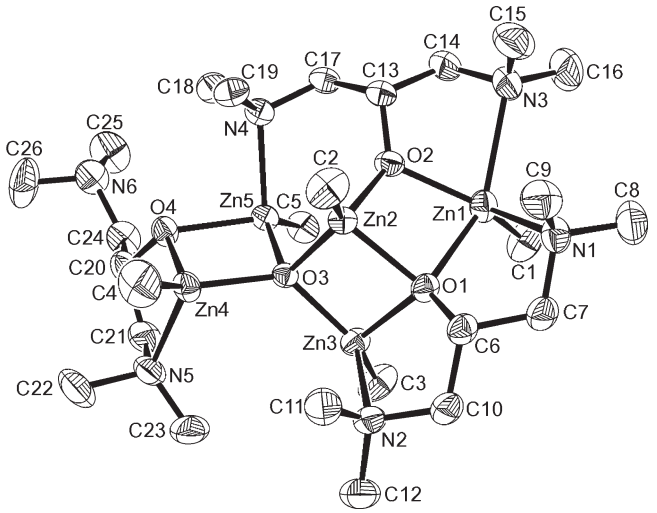

Figure 7. Asymmetric unit of **6** showing the labeling scheme used; thermal ellipsoids are at the 50% probability level. Selected geometric data (Å and deg): Zn(1)−O(1) 2.1839(17), Zn(1)−O(2) 2.0189(18), Zn(1)−N(1) 2.309(2), Zn(1)−N(3) 2.434(2), Zn(2)−O(1) 2.0899(18), Zn(2)−O(2) 2.0007(16), Zn(2)−O(3) 1.9712(15), Zn(3)−O(1) 2.0848(16), Zn(3)−O(3) 1.9539(17), Zn(3)−N(2) 2.236(2), Zn(4)−O(3) 1.9678(16), Zn(4)−O(4) 2.0262(16), Zn(4)−N(5) 2.202(2), Zn(5)−O(3) 2.0019(15), Zn(5)−O(4) 2.0755(17), Zn(5)−N(4) 2.184(2); O(1)−Zn(1)−O(2) 77.50(6), N(1)−Zn(1)−N(3) 96.17(9), O(1)−Zn(2)−O(2) 80.13(7), O(1)−Zn(2)−O(3) 87.31(7), O(2)−Zn(2)−O(3) 97.36(7), O(1)−Zn(3)−O(3) 87.91(7), O(3)−Zn(4)−O(4) 88.83(7), O(3)−Zn(5)−O(4) 86.55(6), O(4)−Zn(5)−N(4) 91.50(8), O(3)−Zn(5)−N(4) 110.30(7), Zn(1)−O(1)−Zn(2) 94.35(7), Zn(1)−O(1)−Zn(3) 118.25(7), Zn(1)−O(2)−Zn(2) 102.51(8), Zn(2)−O(3)−Zn(3) 95.96(7), Zn(2)−O(3)−Zn(4) 114.68(8), Zn(2)−O(3)−Zn(5) 108.80(7), Zn(3)−O(3)−Zn(4) 131.50(8), Zn(3)−O(3)−Zn(5) 111.06(8), Zn(4)−O(3)−Zn(5) 94.20(7), Zn(4)−O(4)−Zn(5) 90.30(7).

(O)Zn[pyr-2,5-Ph_2]}$_2$ (Hpyr-2,5-Ph_2 = 2,5-diphenylpyrrole),[31] [Zn_3{Ph_2PC(H)Py}$_4$(O)],[32] [$Zn_6(O)_2$(FDCA)$_5$(H_2O)(DMF)] (FDCA = 1,10-ferrocene dicarboxylate),[33] and [$Zn_3(O)_2(H_2L)$-$(L)_2$] [H_2L = *N,N*-bis(5-ethyl-1,3,4-thiadiazol-2-yl)-2,6-pyridinedicarboxamide].[34] The μ_3-OZn bond lengths in **7** [1.896(3)−1.903(3) Å] are shorter than the analogous bonds involving μ_4-OZn_4 in **6** [1.9539(17)−2.0019(15) Å] but longer than those for linear μ_2-OZn_2 [1.854(1) Å] in the highly hindered compound [($Tp^{Cum,\ Me}$)Zn]$_2$(O) [$Tp^{Cum,\ Me}$ = hydrotris(3-*p*-cumenyl-5-methylpyrazolyl)borate].[35] The ligands fall into two groups; those based on O(1) and O(4) are μ_2,κ^2-O,N, while the O(2),O(3)-centered ligands are both μ_2,κ^3-O,N,N in their bonding modes.

The details of how these decomposition products are formed are a matter for conjecture, but the structural elements that make up **6** and **7** provide an indication. Compound **6** consists of a six-membered $(MeZn)_3(bdmap)_2O$ fragment that can be traced back to the homolysis of the O−O bond in **4** leading to, initially, the radical [$(MeZn)_3(bdmap)_2(O^{\bullet})$], which forms either **5** by $H^{\bullet}$ abstraction or **6** by another route. The remaining

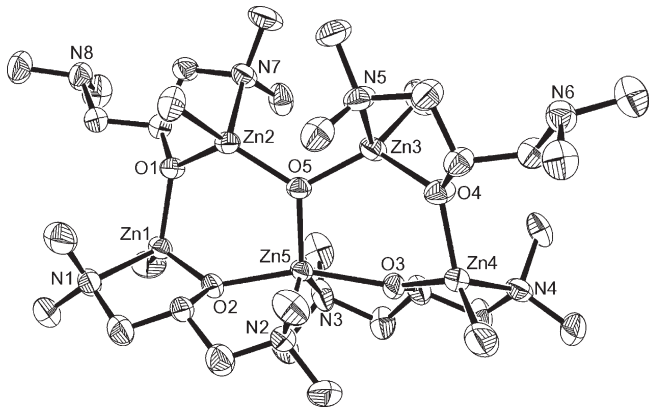

Figure 8. Asymmetric unit of **7** showing the labeling scheme used; thermal ellipsoids are at the 40% probability level. Only the major component of the disorder in the bdmap ligand based on O3 is shown; the molecule of solvation (toluene) has also been omitted for clarity. Selected geometric data (Å and deg): Zn(1)−O(1) 1.952(3), Zn(1)−O(2) 1.988(3), Zn(1)−N(1) 2.184(4), Zn(2)−O(1) 2.063(3), Zn(2)−O(5) 1.896(3), Zn(2)−N(7) 2.240(3), Zn(3)−O(4) 2.051(3), Zn(3)−O(5) 1.899(3), Zn(3)−N(5) 2.222(4), Zn(4)−O(3) 1.996(3), Zn(4)−O(4) 1.944(3), Zn(4)−N(4) 2.06(3), Zn(5)−O(2) 2.095(3), Zn(5)−N(3) 2.161(4), Zn(5)−O(3) 2.112(3), Zn(5)−N(2) 2.195(4), Zn(5)−O(5) 1.903(3); O(1)−Zn(1)−O(2) 97.84(11), O(1)−Zn(2)−O(5) 115.98(12), O(4)−Zn(3)−O(5) 119.60(12), O(3)−Zn(4)−O(4) 94.55(12), O(2)−Zn(5)−O(3) 160.36(11), O(2)−Zn(5)−O(5) 100.17(11), O(3)−Zn(5)−O(5) 99.43(12), N(2)−Zn(5)−N(3) 121.77(16).

part of **6**, $(MeZn)_2$(bdmap), is most simply rationalized by reaction of [$(MeZn)_3(bdmap)_2(O^{\bullet})$] with half of dimeric **2** in a process that results in loss of $Me^{\bullet}$:

$$(MeZn)_3(bdmap)_2O\bullet + MeZn(bdmap)\cdot ZnMe_2 \xrightarrow{-Me\cdot} (MeZn)_5(bdmap)_3O\ (\mathbf{6})$$

This is the general type of reaction sequence that others have used to explain the formation of zincoxane products from zinc peroxide intermediates. For example,[13,17]

$$Me_2Zn(^t\mathrm{BuDAB}) \xrightarrow{O_2} Me(MeOO)Zn(^t\mathrm{BuDAB}) \xrightarrow[-MeO\cdot,\ -Me\cdot]{Me_2Zn(^t\mathrm{BuDAB})} [MeZn(OOMe)]_2[MeZnOZnMe(^t\mathrm{BuDAB})]_2$$

$$EtZn(Pyr\text{-}pyr) \xrightarrow{O_2} [EtOOZn(Pyr\text{-}pyr)][EtZn(Pyr-pyr)]_n \xrightarrow{-EtO\cdot} \xrightarrow{-Et\cdot} Zn_4(Pyr\text{-}pyr)_6O$$

However, the fact that the decomposition products have been observed from reactions in which **4** is formed *in situ* from adduct **2** (which contains excess $ZnMe_2$) and also from isolated **4** (which has no excess $ZnMe_2$) means that the radical derived from **4** must react at zinc of a second species but not with loss of $Me^{\bullet}$, as all the zinc centers in **6** retain methyl groups, unless **4** undergoes Schlenk equilibria which generate $ZnMe_2$ *in situ*. Thus, while the decomposition of **4** and formation of **6** do appear to be facilitated by the presence

(31) Zhu, G.; Tanski, J. M.; Parkin, G. *J. Chem. Crystallogr.* **2002**, *32*, 469.
(32) Murso, A.; Stalke, D. *Dalton Trans.* **2004**, 2563.
(33) Kim, Y. S.; Kim, J.; Kim, D.; Chae, H. K. *Chem. Lett.* **2007**, *36*, 150.
(34) Shen, X.-Q.; Yao, H.-C.; Yang, R.; Li, Z.-J.; Zhang, H.-Y.; Wu, B.-L.; Hou, H.-W. *Polyhedron* **2008**, *27*, 203.
(35) Ruf, M.; Vahrenkamp, H. *Inorg. Chem.* **1996**, *35*, 6571.

of $ZnMe_2$, as noted above in the discussion of Figure 4c, it seems likely that the decomposition also involves equilibria of the following kind (L = bdmap):

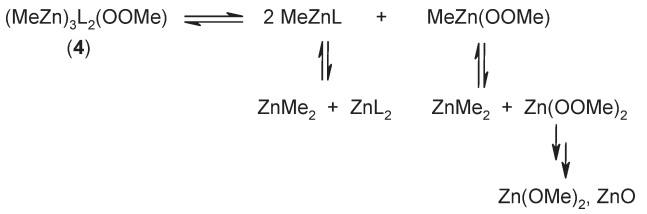

Equilibria of the kind shown above are prevalent in this area of organozinc chemistry, and we have previously shown that $Zn(bdmap)_2$ crystallizes from an aged sample of $[MeZn(bdmap)]_n$, and $EtZn_3(bdmap)_5$ from $[EtZn(bdmap)]_3$ by similar routes.[20] Of the species that are plausibly present in solution, we would expect the order of reactivity to be $ZnMe_2$ > MeZnL > ZnL_2, based on a diminishing number of reactive Zn−Me bonds, the monodentate nature of Me compared to bi/tridentate bdmap, and finally the increased coordination at zinc in $Zn(bdmap)_2$ (CN = 5) in comparison with the two organometallics (CN = 4).[20] In addition, we might expect $Zn(OOMe)_2$ to be highly reactive and arguably be, at least in part, the origin of any insoluble end-products such as $Zn(OMe)_2$ or ZnO.

Conclusions

The reaction of $ZnMe_2$ with Hbdmap in 2:1 ratio forms both $[MeZn(bdmap)\cdot ZnMe_2]_2$ (**2**) and $[MeZn(bdmap)]_3\cdot ZnMe_2$ (**3**) depending on the concentration of the reaction. In the former, the $ZnMe_2$ is coordinated to a free N-donor of the bdmap ligand and rather more loosely to the oxygen of the alkoxide. **2** reacts with O_2 at low temperatures with controlled insertion into one of the Zn−C bonds of the coordinated $ZnMe_2$ group to form the isolable peroxide $[MeZn(bdmap)]_2$-MeZnOOMe (**4**), a reaction that supports the idea that *in situ* formation of a three-coordinate zinc is key to this reaction. **4** decomposes slowly, and the hydroxide $[MeZn(bdmap)]_2$-MeZnOH (**5**), possibly arising from homolysis of the peroxide O−O bond, is isolated. In addition to **5**, two other decomposition products have been unambiguously identified, namely, $(MeZn)_5(bdmap)_3O$ (**6**) and $(MeZn)_4(bdmap)_4ZnO$ (**7**). The formation of these species can be linked to reactions of the hydroxide (**5**), or its associated radical $[MeZn(bdmap)]_2MeZn(O^{\bullet})]$, with species such as $ZnMe_2$ or MeZn(bdmap), present in solution as a result of operating Schlenk equilibria.

Acknowledgment. We thank the EPSRC for a doctoral training award (to N.H.). SAFC Hitech is thanked for a gift of $ZnMe_2$.

Supporting Information Available: This material is available free of charge via the Internet at http://pubs.acs.org. Crystallographic data for the structural analysis (in CIF format) have also been deposited with the Cambridge Crystallographic Data Center, CCDC nos. 698985−698990 and 766016 for **1**−**6** and **7**, respectively. Copies of this information may be obtained from the Director, CCDC, 12 Union Road, Cambridge, CB21EZ, UK (fax: +44-1233-336033; e-mail: deposit@ccdc.cam.ac.uk or www.ccdc.cam.ac.uk).